at 25 °C (1.4–1.7, Table I). Since the kinetic isotope effect on the overall reaction (eq 12) is larger than the kinetic isotope effect found for eq 10, an additional contribution from k_3 is thereby implied, as expected for the making of an H–H (H–D) bond accompanied by the breaking of an Ru–H (Ru–D) bond.

Acknowledgment. This work was supported by grants from the National Science Foundation (CHE 88-00515 and CHE 84-11630).

Synthesis, Structure, and Reactivity of Cluster Complexes Containing the $Pt_3(\mu_3\text{-Sn})$ Unit and a Possible Relationship to Heterogeneous Platinum–Tin Catalysts

Michael C. Jennings, Guy Schoettel, Sujit Roy, and Richard J. Puddephatt*

Department of Chemistry, University of Western Ontario, London, Ontario, Canada N6A 5B7

Graeme Douglas, Ljubica Manojlović-Muir,* and Kenneth W. Muir

Department of Chemistry, University of Glasgow, Glasgow G12 8QQ, Scotland

Received May 7, 1990

The reaction of $[Pt_3(\mu_3\text{-CO})(\mu\text{-dppm})_3]^{2+}$ (**1**), as the PF_6^- salt, with Me_2SnH_2 gave first $[Pt_3(\mu_3\text{-H})(\mu_3\text{-SnMe}_2H)(\mu\text{-dppm})_3]^{2+}$ (**2**) and then $[Pt_3\{\mu_3\text{-SnMe}_2(O_2PF_2)\}(\mu\text{-dppm})_3]^+$ (**3**) while the reaction of **1** with Ph_3SnH gave $[Pt(\mu_3\text{-CO})(\mu_3\text{-SnF}_3)(\mu\text{-dppm})_3]^+$ (**4a**) and $[Pt_3(\mu_3\text{-Cl})(\mu_3\text{-SnF}_3)(\mu\text{-dppm})_3]$ (**5**). Complexes **4a** and $[Pt_3(\mu_3\text{-CO})(\mu_3\text{-SnCl}_3)(\mu_3\text{-dppm})_3]^+$ (**4b**) could also be prepared by reaction of **1** with SnF_3^- and $SnCl_3^-$, respectively. Reaction of **1** with excess SnF_3^- or $SnCl_3^-$ gave $[Pt_3(\mu_3\text{-SnF}_3)_2(\mu\text{-dppm})_3]$ (**6a**) or $[Pt_3(\mu_3\text{-SnCl}_3)_2(\mu\text{-dppm})_3]$ (**6b**), respectively. The structure of **6a** has been determined by X-ray crystallography. Reaction of **4a** with acetylene in CH_2Cl_2 gave an equimolar mixture of $[Pt_3Cl(\mu_3\text{-HCCH})(\mu\text{-dppm})_3]^+$ (**8**) and **6a**, reaction with H_2S gave $[Pt_3H(\mu_3\text{-S})(\mu\text{-dppm})_3]^+$ (**9**) and SnS, and reaction with XyNC (Xy = 2,6-$Me_2C_6H_3$) gave $[Pt_3(\mu_3\text{-SnF}_3)(\text{XyNC})(\mu\text{-dppm})_3]^+$ (**7**), which contains a terminal XyNC ligand. The stability of the $Pt_3(\mu_3\text{-SnX}_3)$ unit, together with the ability of the coordinatively unsaturated Pt_3 clusters to mimic properties of a Pt surface, suggests that heterogeneous Pt–Sn–Al_2O_3 catalysts may contain platinum–tin alloy anchored to the tin(II)–alumina support by similar $Pt_3(\mu_3\text{-Sn})$ linkages. An ESCA study of the complexes suggests that SnF_3^- is a stronger σ-donor than CO but also competes with CO as a π-acceptor ligand.

Introduction

Bimetallic Pt–Sn systems are involved in both homogeneous and heterogeneous catalysis.[1-6] Molecular Pt(II)–Sn(II) complexes take part in homogeneous catalytic hydrogenation, hydroformylation, and isomerization of alkenes.[2-6] Most of these compounds contain the $SnCl_3^-$ ligand.[1-9] Heterogeneous Pt–Sn–Al_2O_3 catalysts are used in re-forming of petroleum since they give higher selectivity for isomerization and aromatization than Pt–alumina catalysts alone. They appear to contain both Sn(0) and Sn(II) species, but the origin of the tin effect is not clearly established.[10-19]

Scheme I

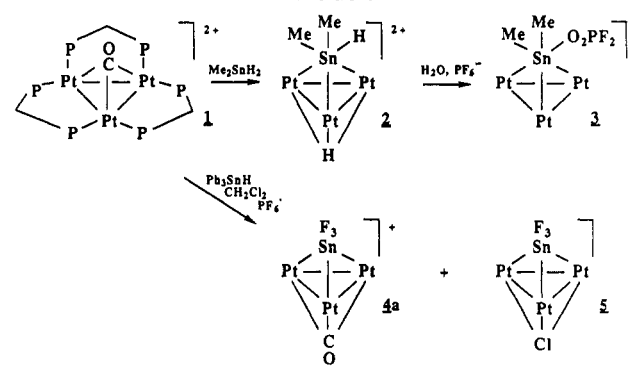

(1) Holt, M. S.; Wilson, W. L.; Nelson, J. H. *Chem. Rev.* **1989**, *89*, 11.
(2) Cramer, R. D.; Jenner, E. L.; Lindsey, R. V., Jr.; Stolberg, U. G. *J. Am. Chem. Soc.* **1963**, *85*, 1691.
(3) Anderson, G. K.; Clark, H. C.; Davies, J. A. *Inorg. Chem.* **1983**, *22*, 427, 434, 439.
(4) Anderson, G. K.; Clark, H. C.; Davies, J. A. *Organometallics* **1982**, *1*, 64.
(5) Hsu, C.; Orchin, M. *J. Am. Chem. Soc.* **1975**, *97*, 3553.
(6) Kawabata, Y.; Hayashi, T.; Ogata, I. *J. Chem. Soc., Chem. Commun.* **1979**, 462.
(7) Herbert, I. R.; Pregosin, P. S.; Ruegger, H. *Inorg. Chim. Acta* **1986**, *112*, 29. Arz, C.; Herbert, I. R.; Pregosin, P. S. *J. Organomet. Chem.* **1986**, *308*, 373.
(8) Albinati, A.; Moriyama, H.; Ruegger, H.; Pregosin, P. S.; Togni, A. *Inorg. Chem.* **1985**, *24*, 4430. Reugger, H.; Pregosin, P. S. *Inorg. Chem.* **1987**, *26*, 2912.
(9) Grossel, M. C.; Moulding, R. P.; Seddon, K. R. *Inorg. Chim. Acta* **1982**, *64*, L275.
(10) Adkins, S. R.; Davis, B. H. *J. Catal.* **1984**, *89*, 371.
(11) Davis, B. H. *J. Catal.* **1976**, *42*, 376; **1977**, *46*, 348.
(12) Burch, R.; Garla, L. C. *J. Catal.* **1981**, *71*, 360.
(13) Davis, B. H.; Westfall, G. A.; Watkins, J.; Pezzarite, J., Jr. *J. Catal.* **1976**, *42*, 247.

0276-7333/91/2310-0580$02.50/0

Since it has been shown that the coordinatively unsaturated cluster complex $[Pt_3(\mu_3\text{-}CO)(\mu\text{-}dppm)_3]^{2+}$ (**1**; dppm = $Ph_2PCH_2PPh_2$) can mimic some of the properties of a platinum surface,[20-23] it was considered that the reactions of **1** with tin(II) species could give some insight into the nature of any Pt–Sn(II) interactions in the supported Pt–Sn–Al_2O_3 catalysts and that studies of the reactivities of the Pt_3Sn clusters so formed might suggest how the "tin effect" operates. This, and the realization that there are very few well-characterized complexes having Pt_2Sn or Pt_3Sn groups,[9,24-28] stimulated the work presented here. A preliminary account of parts of the research has been published.[29]

Results

Synthesis with Organotin Hydrides. Initial attempts to prepare Pt_3Sn complexes were made by reaction of **1** with organotin hydrides. These reactions were generally complex, and in only two cases could products be crystallized and fully characterized (Scheme I).

Reaction of **1** with Me_2SnH_2 gave initially the complex $[Pt_3(\mu_3\text{-}H)(\mu_3\text{-}SnMe_2H)(\mu\text{-}dppm)_3]^{2+}$ (**2**), which was characterized spectroscopically. The complex gave a singlet resonance in the ^{31}P NMR spectrum, with satellites due to coupling to ^{195}Pt that are typical of $Pt_3(\mu\text{-}dppm)_3$ complexes with 3-fold symmetry.[20-22] The $Pt_3(\mu_3\text{-}H)$ resonance in the ^1H NMR spectrum was at δ −3.5 with $^1J(PtH)$ = 414 Hz,[21,30] and the $SnMe_2H$ group was identified by the septet and doublet resonances for the SnH and $SnMe_2$ protons, respectively, due to $^3J(HH)$ = 6.1 Hz.

Complex **2** was short-lived in solution, and recrystallization gave the stable complex $[Pt_3\{\mu_3\text{-}SnMe_2(O_2PF_2)\}(\mu\text{-}dppm)_3]^+$ (**3**). This reaction involves loss of the μ_3-H ligand and replacement of hydrogen in the $SnMe_2H$ group of **2** by the O_2PF_2 group in **3**. In turn, the O_2PF_2 group is clearly formed by tin-catalyzed partial hydrolysis of a PF_6^- counterion. The presence of the O_2PF_2 ligand was first revealed by X-ray crystal structure analysis[29] and then confirmed by the characteristic triplet resonance in the ^{31}P NMR spectrum with $^1J(PF)$ = 970 Hz and by IR bands at 1312 and 1098 (ν(PO)) and 722 cm^{-1} (ν(PF)).[31] The single ^{31}P resonance due to the μ-dppm ligands is an indication that the $SnMe_2X$ ligand, X = PO_2F_2, can rotate rapidly with respect to the Pt_3 triangle, since only 2-fold symmetry is possible in the static structure. Treatment of **1** with Ph_3SnH, followed by slow recrystallization, gave in low yield a crystalline material shown to contain $[Pt_3(\mu_3\text{-}SnF_3)(\mu_3\text{-}CO)(\mu\text{-}dppm)_3][PF_6]$ (**4a**) and $[Pt_3(\mu_3\text{-}SnF_3)(\mu_3\text{-}Cl)(\mu\text{-}dppm)_3]$ (**5**) in the molar ratio 3:1. This formulation was based on an X-ray structure analysis[29] and on identification of chloride by X-ray fluorescence analysis with use of scanning electron microscopy on a single crystal. The presence of the carbonyl ligand in **4a** was independently detected by IR spectroscopy (ν(CO) = 1827 cm^{-1}), and the SnF_3 unit was confirmed by ^{19}F NMR spectra. Clearly, all the phenyl–tin bonds are cleaved in this reaction.

Scheme II

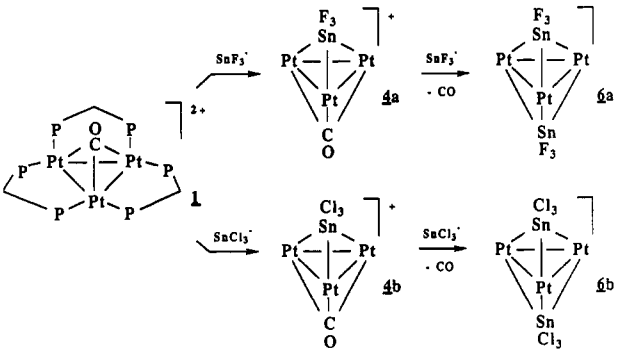

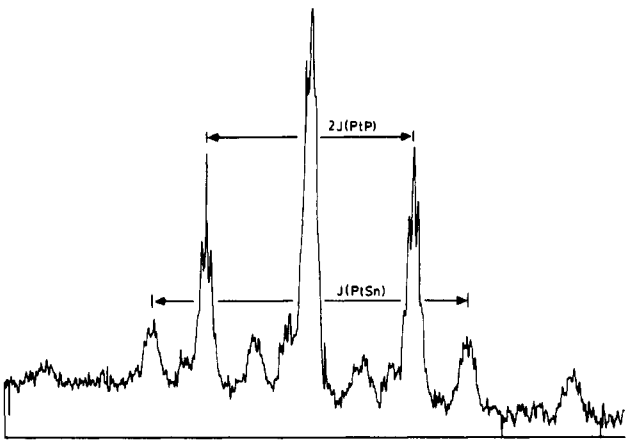

Figure 1. $^{195}Pt\{^1H\}$ NMR spectrum of $[Pt_3(\mu_3\text{-}SnF_3)_2(\mu\text{-}dppm)_3]$. The central triplet resonance arises due to the coupling $^1J(PtP)$, and the inner satellites due to the coupling $^1J(PtSn)$ are indicated.

Since these observations indicated that the complexes were most stable with electronegative substituents on tin, and since preliminary experiments with other organotin hydrides such as Me_3SnH and Ph_2SnH_2 were unsuccessful, another synthetic approach was adopted.

Synthesis from SnF_3^- and $SnCl_3^-$. The synthetic pathways are shown in Scheme II.

Complexes **4a,b** are obtained in good yield by reaction of **1** with 1 equiv of SnF_3^- or $SnCl_3^-$. The SnX_3^- reagents were usually prepared in situ by reaction of SnX_2 with X^-, and this procedure with X = F appeared better than reaction with preformed $Na[SnF_3]$. The presence of a μ_3-CO ligand is indicated by ν(CO) = 1827 and 1763 cm^{-1}, respectively, for **4a,b**. Complex **4a** exhibits the coupling $^1J(PtSn)$ = 14 700 Hz in the ^{195}Pt NMR spectrum. It is interesting that reaction of **4a** with sodium chloride led to substitution of the SnF groups and formation of **4b**, rather than displacement of either the carbonyl or tin(II) ligand.

Reaction of **1** with 2 equiv or more of SnX_3^- gave the neutral, sparingly soluble complexes **6a,b**. These are

(14) Palasov, A.; Bonev, C.; Shopov, D.; Leitz, G.; Sàrkàny, A.; Völter, J. *J. Catal.* **1987**, *103*, 249.
(15) Srinivasan, R.; de Angelis, R. J.; Davis, B. H. *J. Catal.* **1987**, *106*, 449.
(16) Yermakov, Yu. I.; Kuznetsov, B. N. *J. Mol. Catal.* **1980**, *9*, 13.
(17) Sexton, B. A.; Hughes, A. E.; Foger, K. *J. Catal.* **1984**, *88*, 466.
(18) Sachtler, W. M. H.; van Santen, R. A. *Adv. Catal.* **1977**, *26*, 69. Roberti, A.; Ponec, V.; Sachtler, W. M. H. *J. Catal.* **1973**, *28*, 381.
(19) Li, Y.-X.; Zhang, Y.-F.; Klabunde, K. J. *Langmuir* **1988**, *4*, 385.
(20) Ferguson, G.; Lloyd, B. R.; Puddephatt, R. J. *Organometallics* **1986**, *5*, 344.
(21) Lloyd, B. R.; Puddephatt, R. J. *J. Am. Chem. Soc.* **1985**, *107*, 7785.
(22) Lloyd, B. R.; Bradford, A.; Puddephatt, R. J. *Organometallics* **1987**, *6*, 424.
(23) Rashidi, M.; Puddephatt, R. J. *Organometallics* **1988**, *7*, 1636.
(24) Lindsey, R. V., Jr.; Parshall, G. W.; Stolberg, U. G. *Inorg. Chem.* **1966**, *5*, 109.
(25) Guggenberger, L. J. *J. Chem. Soc., Chem. Commun.* **1968**, 512.
(26) Hitchcock, P. B.; Lappert, M. F.; Misra, M. C. *J. Chem. Soc., Chem. Commun.* **1985**, 863.
(27) Campbell, G. K.; Hitchcock, P. B.; Lappert, M. F.; Misra, M. C. *J. Organomet. Chem.* **1985**, *289*, C1.
(28) Bushnell, G. W.; Eadie, D. T.; Pidcock, A.; Sam, A. R.; Holmes-Smith, R. D.; Stobart, S. R.; Brennan, E. T.; Cameron, T. S. *J. Am. Chem. Soc.* **1982**, *104*, 5837.
(29) Douglas, G.; Jennings, M. C.; Manojlović-Muir, Lj.; Muir, K. W.; Puddephatt, R. J. *J. Chem. Soc., Chem. Commun.* **1989**, 159.
(30) Ramachandran, R.; Payne, N. C.; Puddephatt, R. J. *J. Chem. Soc., Chem. Commun.* **1989**, 128.
(31) Addou, A.; Vast, P.; Legrand, P. *Spectrochim. Acta* **1982**, *38A*, 785, 881.

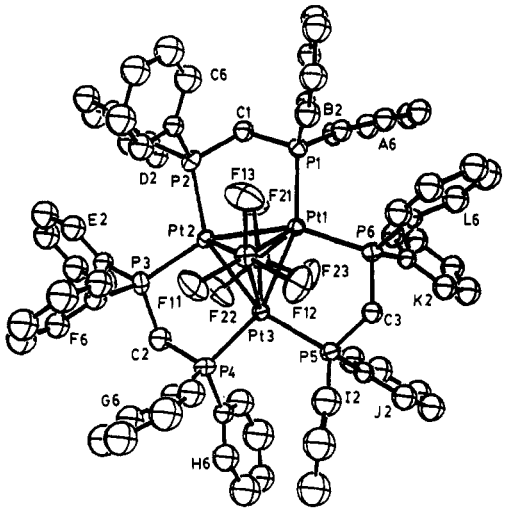

Figure 2. Molecular structure of $Pt_3(\mu_3\text{-}SnF_3)_2(\mu\text{-}dppm)_3$ (**6a**), showing the atomic labeling scheme. In the phenyl rings, the carbon atoms are numbered cyclically, C(n1), ..., C(n6), with n = A, B, ..., L, and the C(n1) atom is bonded to phosphorus. For clarity, only the atoms C(n2) and C(n6) are labeled as n2 or n6.

analogous to the known complex $[Pt_3(\mu_3\text{-}SnCl_3)_2(COD)_3]$ (COD = 1,5-cyclooctadiene).[24,25] Since complexes **6a,b** possess a plane of symmetry containing the $Pt_3P_6C_3$ atoms, the ^1H NMR signal due to the CH_2P_2 protons appears a single resonance, whereas in **4a,b**, which do not have such a plane of symmetry, an "AB" quartet is observed for the nonequivalent CH^AH^B protons. This gives a useful method for distinguishing the two types of complexes. The ^{195}Pt NMR spectrum of **6a** (Figure 1) contained satellites due to $^1J(PtSn)$ = 10 250 Hz, a value significantly lower than in **4a**. Reaction of **6a** with excess chloride gave a mixture of at least five complexes, each giving a singlet in the ^{31}P NMR spectrum in the region expected for $[Pt_3(\mu_3\text{-}SnX_3)_2(\mu\text{-}dppm)_3]$ complexes. Thus, it seems that partial substitution of fluoride for chloride in **6a** occurs to give complexes containing $Pt_3(\mu_3\text{-}SnF_nCl_{3-n})(\mu_3\text{-}SnF_mCl_{3-m})$ groups but that complete substitution to give **6b** does not occur.

Structural Properties of the Pt_3Sn and Pt_3Sn_2 Clusters. The structures of **3** and of **4a** and **5**, in $\mathbf{4a}_{0.75}\mathbf{5}_{0.25}$, have been reported earlier[29] and will not be further described here.

The structure of the Pt_3Sn_2 complex **6a** is shown in Figure 2 and characterized by bond lengths and angles listed in Table I. It contains a triangular arrangement of platinum atoms (Pt–Pt = 2.609 (2), 2.622 (1), and 2.639 (1) Å), with each edge of the triangle bridged by a μ-dppm ligand and each face by a μ_3-SnF_3 ligand. Thus, the Pt_3Sn_2 cluster adopts a slightly distorted trigonal-bipyramidal geometry (Figure 3), with two apical μ_3-SnF_3 ligands in an eclipsed orientation with respect to each other. The stereochemistry of the tin centers is approximately octahedral, each tin(II) ion being bound to three fluorine and three platinum atoms. In the $Pt_3(\mu\text{-}dppm)_3$ fragment the Pt_3P_6 skeleton adopts a somewhat distorted latitudinal M_3P_6 geometry, the largest displacement of a phosphorus atom from the Pt_3 plane being 0.249 (4) Å (Table I). All three Pt_2P_2C rings are in envelope conformations with methylene groups at the "flaps", one of which is pointing toward the Sn(1) and the other two toward the Sn(2) atom (Figure 3). As a result, the $Sn(1)F_3$ ligand is surrounded by four axial phenyl groups (B, C, G, F) and therefore lies in a sterically more crowded environment than the $Sn(2)F_3$ ligand, which is surrounded by two axial phenyl groups only (K, J).

Table I. Selected Paramters of the Molecular Structure of $[Pt_3(\mu_3\text{-}SnF_3)_2(\mu\text{-}dppm)_3]$ (6a)

Bond Lengths (Å)

Pt(1)–Pt(2)	2.639 (1)	Pt(2)–P(3)	2.313 (5)
Pt(1)–Pt(3)	2.609 (2)	Pt(3)–P(4)	2.278 (5)
Pt(2)–Pt(3)	2.622 (1)	Pt(3)–P(5)	2.308 (5)
Pt(1)–Sn(1)	2.746 (2)	Pt(1)–P(6)	2.303 (5)
Pt(2)–Sn(1)	2.801 (2)	Sn(1)–F(11)	1.99 (1)
Pt(3)–Sn(1)	2.783 (2)	Sn(1)–F(12)	1.96 (1)
Pt(1)–Sn(2)	2.808 (2)	Sn(1)–F(13)	1.90 (1)
Pt(2)–Sn(2)	2.699 (2)	Sn(2)–F(21)	1.97 (1)
Pt(3)–Sn(2)	2.830 (2)	Sn(2)–F(22)	1.96 (1)
Pt(1)–P(1)	2.301 (5)	Sn(2)–F(23)	1.90 (1)
Pt(2)–P(2)	2.304 (6)		
P–C(CH_2)	1.81 (2)–1.85 (2)		
P–C(Ph)	1.81 (2)–1.86 (2)		

Bond Angles (deg)

Pt(2)–Pt(1)–Pt(3)	59.9 (1)	Pt(1)–Pt(3)–P(5)	96.5 (2)
Pt(2)–Pt(1)–P(1)	97.6 (2)	Pt(2)–Pt(3)–P(4)	96.4 (2)
Pt(3)–Pt(1)–P(6)	94.5 (2)	P(4)–Pt(3)–P(5)	106.7 (2)
P(1)–Pt(1)–P(6)	108.2 (2)	Pt(1)–Pt(3)–P(4)	156.8 (2)
Pt(2)–Pt(1)–P(6)	154.3 (2)	Pt(2)–Pt(3)–P(5)	156.8 (2)
Pt(3)–Pt(1)–P(1)	156.8 (2)	Sn(1)–Pt(3)–Sn(2)	112.1 (1)
Sn(1)–Pt(1)–Sn(2)	113.9 (1)	Pt(1)–Sn(1)–Pt(2)	56.8 (1)
Pt(1)–Pt(2)–Pt(3)	59.5 (1)	Pt(2)–Sn(1)–Pt(3)	56.0 (1)
Pt(1)–Pt(2)–P(2)	93.3 (2)	Pt(3)–Sn(1)–Pt(1)	56.3 (1)
Pt(3)–Pt(2)–P(3)	94.5 (2)	Pt(1)–Sn(2)–Pt(2)	57.2 (1)
P(2)–Pt(2)–P(3)	112.3 (2)	Pt(2)–Sn(2)–Pt(3)	56.6 (1)
Pt(1)–Pt(2)–P(3)	153.4 (2)	Pt(3)–Sn(2)–Pt(1)	55.1 (1)
Pt(3)–Pt(2)–P(2)	152.8 (2)	P(1)–C(1)–P(2)	113.4 (10)
Sn(1)–Pt(2)–Sn(2)	115.7 (1)	P(3)–C(2)–P(4)	112.9 (10)
Pt(1)–Pt(3)–Pt(2)	60.6 (1)	P(5)–C(3)–P(6)	113.0 (9)
Pt–Pt–Sn	59.2 (1)–64.2 (1)		
P–Pt–Sn	101.9 (2)–115.6 (2)		
Pt–Sn–F(cis)	98.2 (4)–111.3 (4)		
Pt–Sn–F(trans)	152.3 (4)–163.6 (4)		
F–Sn–F	88.7 (6)–91.9 (5)		
Pt–P–C(CH_2)	107.6 (7)–110.9 (6)		
Pt–P–C(Ph)	113.9 (6)–123.4 (4)		
C(CH_2)–P–C(Ph)	100.0 (9)–105.2 (8)		
C(Ph)–P–C(Ph)	99.3 (11)–104.0 (8)		

Displacements of Atoms (Å) from the Plane Defined by Pt(1), Pt(2), and Pt(3)

P(1)	−0.249 (4)	P(4)	−0.148 (5)	C(1)	−0.85 (2)
P(2)	−0.069 (4)	P(5)	0.163 (5)	C(2)	−0.96 (2)
P(3)	−0.238 (5)	P(6)	0.118 (5)	C(3)	0.87 (2)

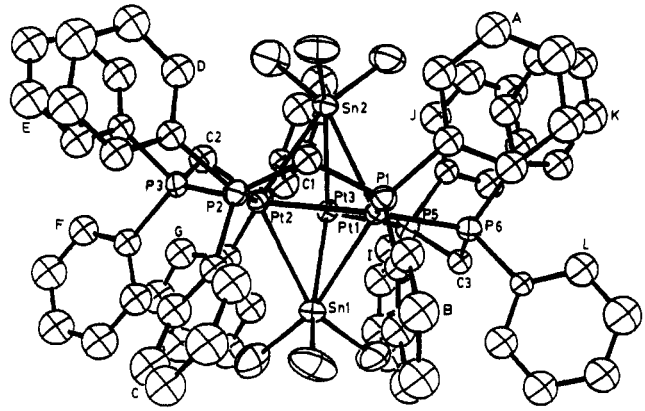

Figure 3. Another view of the structure of $[Pt_3(\mu_3\text{-}SnF_3)_2(\mu\text{-}dppm)_3]$ (**6a**), illustrating the steric environment of the two SnF_3 ligands.

The bond lengths in **6a** are in agreement with those previously observed in the Pt_3Sn clusters **3** and **4a** (Table II). Thus, the mean Pt–Pt distances are nearly the same in the three dppm-bridged clusters (2.620 (8) Å in **3**, 2.639 (3) Å in **4a**, and 2.623 (9) Å in **6a**), but they are all slightly longer than the analogous distance (2.58 (1) Å) in $[Pt_3(\mu_3\text{-}SnCl_3)_2(COD)_3]$ (**10**),[25] though it should be noted that

Table II. Selected Bond Lengths (Å) in dppm-Bridged Clusters with $Pt_3(\mu_3\text{-}Sn)$ Groups

	3	4a	6a	
		Individual Lengths		
Pt(1)–Pt(2)	2.609 (1)	2.639 (3)	2.639 (1)	
Pt(1)–Pt(3)	2.615 (1)		2.609 (2)	
Pt(2)–Pt(3)	2.635 (1)		2.622 (1)	
Pt(1)–Sn	2.766 (2)	2.805 (2)	2.746 (2)	2.808 (2)
Pt(2)–Sn	2.739 (2)		2.801 (2)	2.699 (2)
Pt(3)–Sn	2.702 (2)		2.783 (2)	2.830 (2)
Pt(1)–P	2.272 (4)	2.283 (11)	2.301 (5)	
	2.297 (4)	2.300 (12)	2.303 (5)	
Pt(2)–P	2.284 (4)		2.304 (6)	
	2.264 (4)		2.313 (5)	
Pt(3)–P	2.288 (4)		2.278 (5)	
	2.284 (5)		2.308 (5)	
		Mean Lengths[a]		
Pt–Pt	2.620 (8)	2.639 (3)	2.623 (9)	
Pt–Sn	2.74 (2)	2.805 (2)	2.78 (2)	
Pt–P	2.282 (5)	2.292 (9)	2.301 (5)	

[a] The standard deviation of the mean is the larger of $[\sum(x_i - \bar{x})^2/\{n(n-1)\}]^{1/2}$ and $[\sum 1/\sigma_i^2]^{-1/2}$, where $\bar{x}$ is the mean of n individual x_i values with corresponding standard deviations σ_i.

chemically equivalent Pt–Pt bond lengths in the same molecule may vary by up to 0.03 Å. Greater variation in equivalent Pt–Sn distances (Table II) makes comparison even more difficult. It has been suggested earlier that the trans influence of ligands across the Pt_3 triangle leads to a mutual bond weakening.[21] On this basis, one can predict shorter Pt–Sn distances in the 42-electron cluster **3**, where no trans influence should operate, compared with those in the 44-electron clusters **4a**, **6a**, and **10**. The mean Pt–Sn distances, 2.74 (2) Å in **3**, 2.805 (2) Å in **4a**, 2.78 (2) Å in **6a**, and 2.80 (1) Å in **10**,[25] are consistent with this view, although the variations are nearly of the same order as the experimental errors.

ESCA Study of the Pt_3Sn Clusters. These results for $Pt_3(\mu_3\text{-}SnF_3)$ complexes are shown in Table III, together with some representative literature data. The $Pt(4f_{7/2})$ binding energies for the Pt_3 complexes lie in the range 72.1–72.9 eV. According to previous correlations of $Pt(4f_{7/2})$ binding energy vs platinum oxidation state, these values overlap the ranges for Pt(I) and Pt(II) complexes.[32,33] The *formal* oxidation state of platinum is $+^2/_3$ in these clusters, but formal oxidation states are not particularly informative for such compounds.[32]

When SnF_3^- binds to platinum, the $Sn(3d_{5/2})$ binding energy increases from 486.0 eV in $KSnF_3$ to 486.7 and 486.5 eV in complexes **4a** and **6a**, respectively. This indicates that Sn acts overall as a donor to platinum,[32,34,35] and this interpretation is supported by the observation that addition of SnF_3^- to $[Pt_3(\mu_3\text{-}CO)(\mu\text{-dppm})_3]^{2+}$ to give **4a** causes a decrease in the $Pt(4f_{7/2})$ binding energy from 72.9 to 72.5 eV. Comparison of the $Pt(4f_{7/2})$ binding energies of $[Pt_3(\mu_3\text{-}CO)(\mu_3\text{-}SnF_3)(\mu\text{-dppm})_3]^+$ (72.5 eV) and $[Pt_3(\mu_3\text{-}SnF_3)_2(\mu\text{-dppm})_3]$ (72.7 eV) suggests that SnF_3^- is a slightly stronger donor than CO, but the difference in binding energies is barely statistically significant.

It is interesting that, although the ESCA data show that the electron density at platinum is higher in **4a** than in **1**, the carbonyl stretching frequency of **4a** (1827 cm^{-1}) is higher than that of **1** (1765 cm^{-1}). This unusual observation suggests that the SnF_3^- ligand competes with CO as a π-acceptor and so back-bonding to CO is weaker in **4a** than in **1**. There is a good analogy with the isolobal ligand PF_3, which is comparable to CO as an π-acceptor, due to the presence of electronegative fluoro substituents. The carbonyl stretching frequency for **4b** is 1763 cm^{-1}, consistent with $SnCl_3^-$ being a stronger donor and poorer π-acceptor ligand than SnF_3^-.

Scheme III

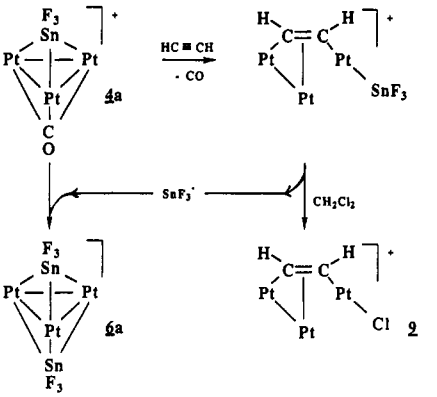

Reactions of the Pt_3Sn Complexes. Complex **4** reacted with XyNC (Xy = 2,6-$Me_2C_6H_3$) with displacement of the carbonyl ligand to give $[Pt_3(\mu_3\text{-}SnF_3)(XyNC)(\mu\text{-dppm})_3]^+$ (**7**; eq 1, dppm ligands omitted).

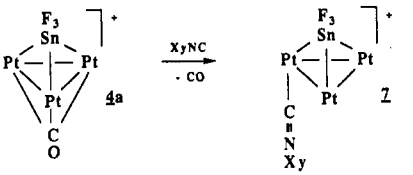

(1)

Complex **7** gives a single ^{31}P resonance and a single ^{195}Pt resonance, whereas three and two such resonances respectively are predicted for the static structure **7**. These spectra thus suggest a complex with 3-fold symmetry and hence a μ_3-XyNC ligand, analogous to structure **4a**. However, the IR spectrum gives $\nu(NC) = 2099$ cm^{-1}, which clearly corresponds to a terminal isocyanide ligand. Therefore, the complex is fluxional such that the xylyl isocyanide ligand can migrate easily around the Pt_3 triangle, perhaps by way of a transition state with a μ_3-XyNC ligand. This type of fluxionality has been observed in several related complexes, including examples of phosphine ligand fluxionality.[36] The fluxionality was not frozen out at −82 °C, indicating a particularly low activation energy for the process.

Reaction of complex **4a** with H_2S gave the known complex $[Pt_3H(\mu_3\text{-}S)(\mu\text{-dppm})_3]^+$ (**8**)[37] and tin(II) sulfide.

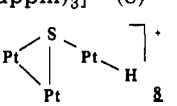

Thus, the SnF_3^- ligand is displaced from platinum. In the reaction of **4a** with acetylene in CH_2Cl_2 solution, the products were $[Pt_3(\mu_3\text{-}SnF_3)_2(\mu\text{-dppm})_3]$ (**6a**) and $[Pt_3Cl(\mu_3\text{-}HCCH)(\mu\text{-dppm})_3]^+$ (**9**).[38] In this case, it is probable

(32) Parshall, G. W. *Inorg. Chem.* **1972**, *11*, 433.
(33) Bancroft, G. M.; Chan, T.; Puddephatt, R. J. *Inorg. Chim. Acta* **1981**, *53*, L119.
(34) Grutsch, P. A.; Zeller, M. V.; Fehlner, T. P. *Inorg. Chem.* **1973**, *12*, 1431.
(35) Starzewski, K. A. O.; Pregosin, P. S. In *Catalytic Aspects of Metal Phosphine Complexes*; Alyea, E. C., Meek, D. W., Eds.; Advances in Chemistry Series 196; American Chemical Society: Washington, D.C., 1982; p 23.
(36) Bradford, A. M.; Jennings, M. C.; Puddephatt, R. J. *Organometallics* **1988**, *7*, 792.
(37) Jennings, M. C.; Payne, N. C.; Puddephatt, R. J. *Inorg. Chem.* **1987**, *26*, 3776.
(38) Douglas, G.; Manojlović-Muir, Lj.; Muir, K. W.; Rashidi, M.; Anderson, C. M.; Puddephatt, R. J. *J. Am. Chem. Soc.* **1987**, *109*, 6527.

Table III. Experimental Binding Energies (eV)[a]

compd	Pt(4f$^{7/2}$)	P(2p)	Sn(3d$_{5/2}$)	C(1s)	ref
$[Et_4N]SnCl_3$			485.7		32
$KSnF_3$			486.0		34
dppm		131.1		282.6	*b*
$[PtCl_2(dppm)]$	73.4	132.1		283.5	*b*
cis-$[PtCl(SnCl_3)(PPh_3)_2]$		132.5	486.8		35
trans-$[PtCl(SnCl_3)(PEt_3)_2]$	73.3	131.6	487.2		35
$[PtCl(SnCl_3)(dppe)]$			485.7	284.0	34
$[Pt_2Cl_2(\mu\text{-dppm})_2]$	72.4				33
$[Pt_2(\mu\text{-}SPPh_2)_2(PPh_3)_2]$	72.0				33
$[Pt_3(CO)(dppm)_3]X_2$[c]	72.9	131.5		283.5, 281.5	*b*
$[Pt_3(CO)(SnF_3)(dppm)_3]X$	72.5	131.6	486.7	283.3, 281.6	*b*
$[Pt_3(CO)(Cl)(dppm)_3]X$	72.1	131.5		283.5, 281.6	*b*
$[Pt_3(SnF_3)_2(dppm)_3]$	72.7	131.7	486.5	283.1	*b*
$[Et_4N]_4[Pt_3Sn_8Cl_{20}]$	72.9		487.3		32

[a] Corrected with respect to C(1s) BE of 285.0 eV. [b] This work. [c] X = $[PF_6]$.

that the initially formed complex is $[Pt_3(\mu_3\text{-HCCH})(SnF_3)(\mu\text{-dppm})_3]^+$, which then loses the terminal SnF_3^- ligand to give $[Pt(\mu_3\text{-HCCH})(\mu\text{-dppm})_3]^{2+}$. This then reacts with the chlorinated sovlent to give **9**; the liberated SnF_3^- reacts with **4a** to give **6a**. Complex **6a** is unreactive toward H_2S, acetylene, or xylyl isocyanide, presumably because access to the Pt_3 triangle is blocked by the two SnF_3 groups.

Discussion

The most novel aspect of the present work is the isolation and characterization of the complexes **4a** and **6a**, which contain the $Pt_3(\mu_3\text{-}SnF_3)$ unit. The SnF_3 unit binds tightly in complex **6a**, and no reactivity at the Pt_3 triangle was found. Complex **4a** is more reactive, but this is probably due to accessibility of the Pt_3 triangle on the carbonyl side. In the reaction of **4a** with XyNC, this is obvious, but the reactions with acetylene and H_2S are less clear. We propose that these reactions initially occur to give complexes with terminal Pt–SnF_3 groups, such as $[Pt_3(\mu_3\text{-HCCH})(SnF_3)(\mu\text{-dppm})_3]^+$, but that the terminal Pt–SnF_3 group is labile and easily gives free SnF_3^-. Consistent with this hypothesis is our failure to synthesize any simple, mononuclear complexes containing Pt–SnF_3 groups, though analogous Pt–$SnCl_3$ groups are easily prepared.[1-9] Indeed, no transition-metal complexes of SnF_3^- appear to have been reported previously.[29] Our work suggests that $M_3(\mu_3\text{-}SnF_3)$ complexes may be generally accessible.

The tin(II) ligands studied in this work form $Pt_3(\mu_3\text{-}SnX_3)$ groups, both in the 42-electron cluster **3** and the 44-electron clusters **4** and **6**. The tin(II) ligand may be the more electron-donating $Me_2Sn(O_2PF_2)^-$ or the more electron-withdrawing $SnCl_3^-$ or SnF_3^-. The existence of a bridging $Pt_3(\mu_3\text{-}SnCl_3)$ unit had been established much earlier by the Du Pont group in the cluster complex $[Pt_3(\mu_3\text{-}SnCl_3)_2(COD)_3]$.[24,25] Together, these results may give some insight into the mode of interaction in Pt–Sn–Al_2O_3 catalysts. Davis has suggested that these heterogeneous catalysts contain a layer of tin(II) aluminate covering the alumina in an "eggshell" fashion, with the Pt atoms bound to the tin eggshell. It now seems likely that this binding involves $Pt_3(\mu_3\text{-Sn})$ linkages at the interface, and a strong binding interaction is predicted. Of course, this does not answer the questions of why the catalysts are more selective and what role the tin(0) plays, but it does indicate how the platinum catalyst may be anchored and gives some preliminary indication of how the tin(II) may affect the electronic properties of the platinum catalyst. Caution is, of course, necessary since these clusters are very crude models for a platinum surface. It is also noted that binding of SnF_3^- to $[Pt_3(\mu_3\text{-CO})(\mu\text{-dppm})_3]^{2+}$ causes an increase in ν(CO) for the μ_3-CO ligand, whereas Pt–Sn catalysts give a decrease in ν(CO) for the terminal carbonyl chemisorbed on the catalyst surface.

Experimental Section

^1H and ^{19}F NMR spectra were recorded by using a Varian XL-200 NMR spectrometer, and ^{31}P and ^{195}Pt NMR spectra were recorded by using a Varian XL-300 NMR spectrometer. References were TMS (^1H), $CFCl_3$ (^{19}F), H_3PO_4 (^{31}P), and aqueous $K_2[PtCl_4]$ (^{195}Pt). IR spectra were recorded on a Bruker IR/32 FTIR spectrometer, and FAB mass spectra were recorded on a Finnigan MAT 8230 mass spectrometer on mulls in oxalic acid/3-mercapto-1,2-propanediol. Elemental analyses were carried out by Guelph Chemical Laboratories. Complex **1** was prepared as described elsewhere.[20]

$[Pt_3(\mu_3\text{-}SnMe_2H)(\mu_3\text{-H})(\mu\text{-dppm})_3][PF_6]_2$ ($2[PF_6]_2$). An acetone solution of **1** (94.7 mg, 46.1 μmol) in a Schlenk tube was degassed by using a freeze–pump–thaw cycle. Excess Me_2SnH_2 was condensed into the Schlenk tube at −78 °C, and the excess was pumped off immediately after the orange solution had turned red. The solvent was removed under reduced pressure, yielding a red-orange solid. An NMR sample of the product was prepared under a dry, oxygen-free atmosphere and gave the following NMR data: $\delta(^1H)$ = −3.5 [sept, 1 H, ^1J(PtH) = 414 Hz, ^2J(PH) = 20 Hz, $Pt_3(\mu_3\text{-H})$], 1.1 [d, 6 H, ^3J(HH) = 6.1 Hz, $HSn(CH_3)_2$], 3.9 [sept, 1 H, ^1J(SnH) = 122 Hz, ^3J(HH) = 6.1 Hz, $HSn(CH_3)_2$]; $\delta(^{31}P)$ = −12.2 [s, ^1J(PtP) = 3120 Hz, ^2J(PtP) = 236 Hz, ^3J(PP) = 116 Hz]. The product could not be isolated as a pure solid due to its thermal instability.

$[Pt_3(\mu_3\text{-}SnMe_2\{OPOF_2\})(\mu\text{-dppm})_3][PF_6]$ ($3[PF_6]$). An acetone (10 mL) solution of **1** (72.0 mg, 35.0 μmol) in a Schlenk tube was degassed at −30 °C by using a freeze–pump–thaw cycle. Excess dimethyltin dihydride was frozen into the reaction vessel, and the solution was stirred for 1 min at −30 °C, although the solution had changed color from orange to red immediately. The unreacted Me_2SnH_2 and the acetone were removed under reduced pressure as the solution was warmed to ambient temperature, giving a pale brown solid. An NMR solution was prepared under a nitrogen atmosphere, and the following data were collected: $\delta(^1H)$ = 0.46 [t, 6 H, ^2J(SnH) = 48 Hz, ^3J(PtH) = 4.4 Hz, $(CH_3)_2Sn$]; $\delta(^{31}P)$ = −16.2 [s, 6 P, ^1J(PtP) = 3260 Hz, ^2J(PtP) = 120 Hz, ^3J(PP) = 140 Hz, dppm], −30.3 [t, 1 P, ^1J(PF) = 970 Hz, O_2PF_2]; $\delta(^{195}Pt)$ = −2501 [t, ^1J(PtP) = 3260 Hz, Pt]; IR (Nujol) ν(P=O) = 1312 cm^{-1}, ν(P—O) = 1098 cm^{-1} ν(PF) = 722 cm^{-1}. Recrystallization by slow diffusion of pentane into an acetone solution of **3** afforded black/yellow dichroic crystals in small yield, and their structure was determined by X-ray diffraction.[29]

$[Pt_3(\mu_3\text{-CO})(\mu\text{-dppm})_3][PF_6]_2$ + Ph_3SnH ($(4a[PF_6])_{0.75}5_{0.25}$). To a Schlenk tube containing **1** (61.4 mg, 30.0 μmol) in CH_2Cl_2 (5 mL) was added Ph_3SnH (8.1 μL, 32 μmol). The pale orange solution darkened immediately. The solution was evaporated to dryness after 5 min, and the product was washed with diethyl ether to yield a pale brown microcrystalline solid (68%): IR (Nujol) ν(CO) = 1824 cm^{-1}. Recrystallization from acetone/pentane afforded a small yield (15%) of orange cubes. Scanning electron microscopy of a single crystal verified that chlorine was present, and the structure was determined by X-ray diffraction.[29]

$[Pt_3(\mu\text{-dppm})_3(\mu_3\text{-CO})(\mu_3\text{-SnF}_3)][PF_6]$ (4a[PF_6]). To a solution of 1 (100 mg, 48.6 μmol) in THF (10 mL) was added a suspension of an equimolar mixture of NaF (2.04 mg) and SnF_2 (7.62 mg) in THF (10 mL). To prevent formation of **6a**, an atmosphere of CO was maintained during the overnight reaction. The solvent was removed, and the pure pale orange compound **4a** (90%) was obtained by precipitation from CH_2Cl_2 solution with diethyl ether: mp 185 °C dec; IR (Nujol) ν(CO) = 1827 cm^{-1}. NMR data (CD_2Cl_2): $\delta(^1H)$ = 5.12 [d, 3 H, ^2J(HH) = 12 Hz, C*H*^{a}H^b], 5.96 [d, 3 H, ^2J(HH) = 12 Hz, ^3J(PtH) = 84 Hz, CH^a*H*^{b}]; $\delta(^{195}Pt)$ = −2575 [tq, 3 Pt, ^1J(PtP) = 3675 Hz, ^2J(PtF) = 109 Hz, ^1J(SnPt) = 14 700 Hz, Pt]; $\delta(^{119}Sn)$ = −320 [m, $^1J(^{119}SnF)$ = 4146 Hz, SnF_3]. Anal. Calcd for $C_{76}H_{66}Pt_3SnP_7F_9O$: C, 43.74; H, 3.19. Found: C, 43.78; H, 3.66. The sample was stirred, in acetone, under an atmosphere of ^{13}CO for 16 h to give the ^{13}CO-labeled complex: $\delta(^{13}CO)$ = 198 [m, 1 C, ^1J(PtC) = 650 Hz, Pt_3CO], $\delta(^{19}F)$ = −73.5 [d, 6 F, ^1J(PF) = 711 Hz, PF_6], −77.0 [m, 3 F, ^2J(PtF) = 118 Hz, ^3J(CF) = 23 Hz, SnF_3]; $\delta(^{31}P)$ = −1.1[s, ^1J(PtP) = 3684, ^3J(PP) = 156].

$[Pt_3(\mu\text{-dppm})_3(\mu_3\text{-CO})(\mu_3\text{-SnCl}_3)][PF_6]$ (4b[PF_6]). The cluster **4b** was obtained and purified by the same procedure as **4a**: quantities 1 (100 mg) with $SnCl_2{\cdot}2H_2O$ (11 mg) and NaCl (3 mg); yield 83%. IR (Nujol): ν(CO) = 1763 cm^{-1}. $\delta(^1H)$ = 5.60 [d, 3 H, ^2J(HH) = 7 Hz, C*H*^{a}H^b], 5.82 [d, 3 H, ^2J(HH) = 7 Hz, CH^a*H*^{b}]. $\delta(^{31}P)$ = −12.3 [s, ^1J(PtP) = 3703 Hz, ^3J(PP) = 161 Hz].

$[Pt_3(\mu_3\text{-SnF}_3)_2(\mu\text{-dppm})_3]$ (6a). A suspension of NaF (6 mg) and SnF_2 (20 mg) in dry THF was added to a solution of 1 (100 mg) in THF. After an overnight reaction, the solution was evaporated and the powder obtained was washed with acetone, yielding **6a** as a yellow powder (83%): mp 250 °C dec; IR (Nujol) no ν(CO) band; $\delta(^1H)$ = 5.89 [t, 6 H, ^2J(PH) = 20 Hz, CH_2]; $\delta(^{19}F)$ = −73.7 [m, 6 F, average of $^1J(^{117}SnF)$ and $^1J(^{119}SnF)$ = 3680 Hz, ^2J(PtF) = 142 Hz, SnF_3]; $\delta(^{31}P)$ = −2.6 [s, ^1J(PtP) = 3310 Hz, ^3J(PP) = 180 Hz, ^2J(PPt) = 25 Hz]; $\delta(^{119}Sn)$ = −354 [q, 2 Sn, ^1J(SnF) = 5200 Hz, SnF_3]; $\delta(^{195}Pt)$ = −2188 [m, ^1J(PtP) = 3350 Hz, ^1J(PtSn) = 10 250 Hz, Pt_3]. FAB MS: calcd for $[Pt_3Sn_2F_6(dppm)_3]^+$ *m/e* 2090, $[Pt_3Sn_2F_5(dppm)_3]^+$ *m/e* 2071, $[Pt_3SnF_3(dppm)_3]^+$ *m/e* 1914; found *m/e* 2090, 2069, 1913. Anal. Calcd for **6a**·$2CH_2Cl_2$, $C_{77}H_{70}Pt_3Sn_2Cl_4P_6F_6$: C, 40.93; H, 3.12. Found: C, 40.83; H, 3.15.

$[Pt_3(\mu\text{-dppm})_3(\mu_3\text{-SnCl}_3)_2]$ (6b). This was prepared in a similar way: quantities 1 (100 mg), $SnCl_2{\cdot}2H_2O$ (30 mg), and NaCl (10 mg); yield 85%; mp 230 °C dec. Anal. Calcd for **6b**·$2CH_2Cl_2$, $C_{77}H_{70}Pt_3Sn_2Cl_{10}P_6$: C, 39.21; H, 2.99. Found: C, 38.55; H, 3.14. $\delta(^1H)$ = 6.03 [t, 6 H, ^2J(PH) = 19 Hz, CH_2]; $\delta(^{31}P)$ = −7.6 [s, ^1J(PtP) = 3240 Hz, ^3J(PP) = 171 Hz, ^2J(PPt) = 24 Hz]. FAB MS: calcd for $[Pt_3Sn_2Cl_6(dppm)_3]^+$ *m/e* 2188, $[Pt_3SnCl_3(dppm)_3]^+$ *m/e* 1963; found *m/e* 2189, 1964.

$[Pt_3(\mu\text{-dppm})_3(\mu_3\text{-SnF}_3)(XyNC)][PF_6]$ (7[PF_6]). XyNC (6.28 mg) was added to a solution of **4a** (100 mg) in CH_2Cl_2. CO was evolved. Recrystallization from acetone/pentane gave red crystals of 7. IR (Nujol): ν(C≡N) = 2099 cm^{-1}, no ν(CO) band. $\delta(^1H)$ = 6.20 [d, 3 H, ^2J(H^{a}H^b) = 12 Hz, ^3J(PtH^a) = 96 Hz, C*H*^{a}H^b], 5.13 [d, 3 H, ^2J(H^{a}H^b) = 12 Hz, ^3J(PtH^b) = 40 Hz, CH^a*H*^{b}]. $\delta(^{31}P)$ and −82 °C) = −10.8 [s, ^1J(PtP) = 3306 Hz, ^2J(PtP) = 43 Hz, ^3J(PP) = 197 Hz] (room temperature and −82 °C). $\delta(^{195}Pt)$ = −2470 [tq, ^1J(PtP) = 3314 Hz, ^1J(PtSn) = 10 750 Hz, ^2J(PtF) = 187 Hz]. FAB MS: calcd for $[Pt_3Sn(dppm)_2CNXy]^+$ *m/e* 1981, $[Pt_3Sn(dppm)_3]^+$ *m/e* 1857; found *m/e* 2034, 1981, 1893, 1857. Anal. Calcd for $Pt_3C_{84}H_{75}P_7SnF_9N$: C, 46.06; H, 3.41. Found: C, 45.82; H, 3.32.

Reaction of 4a with Acetylene. In a typical reaction, **4a** (60 mg) in CD_2Cl_2 (0.5 mL) in an NMR tube was left under 1 atm of acetylene for 10 h. The known cluster **9** and complex **6a** were formed in equimolar amounts and were characterized[38] by their ^1H and ^{31}P NMR spectra.

Reaction of 4a with H_2S. A solution of **4a** (60 mg) in CD_2Cl_2 (0.5 mL) was allowed to stand under 1 atm of H_2S for 5 min. A gold precipitate formed, which was removed by filtration and analyzed by X-ray fluorescence as SnS. The cluster in solution was isolated and characterized as **8** by its ^1H and ^{31}P NMR spectra.[37]

X-ray Crystal Structure Analysis of $[Pt_3(\mu_3\text{-SnF}_3)_2(\mu\text{-dppm})_3]{\cdot}3CH_2Cl_2$ (6a·$3CH_2Cl_2$). Orange crystals of the title compound were obtained from a CH_2Cl_2 solution. All X-ray measurements were made with graphite-monochromated molybdenum radiation and an Enraf-Nonius CAD4 diffractometer.

Table IV. Crystallographic Data for $[Pt_3(\mu_3\text{-SnF}_3)_2(dppm)_3]{\cdot}3CH_2Cl_2$ (6a·$3CH_2Cl_2$)

empirical formula	$C_{78}H_{72}Cl_6F_6P_6Pt_3Sn_2$
fw	2344.6
space group	$P\bar{1}$
a, Å	13.002 (3)
b, Å	15.027 (3)
c, Å	21.744 (5)
α, deg	83.05 (2)
β, deg	77.29 (2)
γ, deg	78.30 (2)
V, Å^3	4045 (2)
Z	2
d_{calc}, g cm^{-3}	1.925
cryst dimens, mm	0.36 × 0.24 × 0.16
temp, °C	19
radiation (wavelength, Å)	Mo Kα (0.710 69)
μ(Mo Kα), cm^{-1}	62.1
data collecn range (1θ), deg	4–46
abs factors (on *F*)	0.69–1.39
no. of unique rflns	6860
with *I*	vge 3σ(*I*)
no. of params refined	372
R^a	0.051
$R_w{}^b$	0.059
Largest param shift/esd (final cycle)	0.19
largest peak in final Δ*F* map, e Å^{-3}	3.2

$^aR = \sum||F_o| - |F_c||/|F_o|$. $^bR_w = [\sum w(|F_o| - |F_c|)^2/\sum w|F_o<<^2]^{1/2}$, $w = 1/\sigma^2(|F_o|)$.

The unit cell constants (Table IV) were determined by a least-squares treatment of 22 reflections with $11 < \theta < 16°$. A systematic investigation of the diffraction pattern revealed a primitive crystal lattice with the $\bar{1}$ Laue symmetry. The space group $P\bar{1}$ was confirmed by a successful structure analysis.

Intensities of 12 311 reflections with $4 \le 2\theta \le 46°$ were measured by continuous $\theta/2\theta$ scans. The scan widths in θ were 0.90°, and the scan speeds were adjusted to give $\sigma(I)/I \le 0.03$, subject to a time limit of 60 s. Intensities of two strong reflections, remeasured every 2 h, showed only random fluctuations not exceeding 2% of their mean values. The integrated intensities, derived in the usual manner,[39] were corrected for Lorentz, polarization, and absorption effects, the last correction being made by an empirical method at the conclusion of isotropic refinement.[40] A total of 2191 symmetry-related reflections were averaged to give 1095 independent ones and an *R*(internal) value of 0.034. Only 6860 unique reflections, for which $I \ge 3\sigma(I)$, were used in the crystal structure analysis.

The structure was solved by the heavy-atom method. The positions of the metal atoms were found from a Patterson function and those of the remaining non-hydrogen atoms from difference electron density maps. The hydrogen atoms were included in the structural model in calculated positions, with C–H fixed at 1.0 Å and *U*(isotropic) at 0.075 Å^2.

At later stages of analysis, the difference electron density maps revealed the presence of an ordered CH_2Cl_2 solvent molecule (atoms C(4), Cl(1), and Cl(2) in Table V). They also showed two well-separated regions of high electron density, each with five peaks of 8–9 e Å^{-3}. These peaks were assigned to ten chlorine atoms (ClS(11)–ClS(25)), each with *U*(isotropic) constrained to 0.16 Å^2 and an occupancy parameter allowed to vary; the final values of these parameters (Table V) were found indicative of the presence of two highly disordered solvent molecules.

The structural model was refined by minimizing the function $\sum w(|F_o| - |F_c|)^2$, with $w = \sigma^{-2}(|F_o|)$. Only the platinum, tin, phosphorus, fluorine, and Cl(1) and Cl(2) atoms were refined with anisotropic displacement parameters. The 12 phenyl rings were constrained to D_{6h} symmetry and C–C = 1.38 Å, but the isotropic

(39) Manojlović-Muir, Lj.; Muir, K. W. *J. Chem. Soc., Dalton Trans.* **1974**, 2427.
(40) Walker, N.; Stuart, D. *Acta Crystaallogr., Sect. A: Found. Crystallogr.* **1983**, *A39*, 158.

Table V. Fractional Atomic Coordinates and Displacement Parameters (Å²) for $[Pt_3(\mu_3\text{-}SnF_3)_2(\mu\text{-}dppm)_3]\bullet 3CH_2Cl_2$ ($6a\bullet 3CH_2Cl_2$)

atom[a]	x	y	z	U	atom[a]	x	y	z	U
Pt(1)	0.19606 (5)	0.11103 (5)	0.20386 (3)	0.024[b]	C(F1)	0.3216 (19)	0.2709 (12)	0.4132 (8)	0.039 (5)
Pt(2)	0.29846 (5)	0.13848 (5)	0.29008 (3)	0.025	C(F2)	0.2218 (16)	0.2547 (15)	0.4443 (5)	0.054 (6)
Pt(3)	0.22125 (5)	0.27533 (5)	0.21642 (3)	0.026	C(F3)	0.1748 (10)	0.2905 (10)	0.5015 (8)	0.074 (7)
Sn(1)	0.07564 (9)	0.19459 (9)	0.30860 (6)	0.033	C(F4)	0.2278 (19)	0.3425 (12)	0.5276 (8)	0.071 (7)
Sn(2)	0.40535 (9)	0.14772 (9)	0.16875 (6)	0.032	C(F5)	0.3276 (16)	0.3587 (15)	0.4965 (5)	0.070 (7)
Cl(1)	−0.2837 (7)	0.3617 (7)	0.1717 (4)	0.124	C(F6)	0.3745 (10)	0.322((10)	0.4393 (8)	0.049 (5)
Cl(2)	−0.2123 (9)	0.3359 (7)	0.0404 (5)	0.152	C(G1)	0.2046 (20)	0.4523 (10)	0.3164 (10)	0.047 (5)
P(1)	0.2272 (3)	−0.0458 (3)	0.2164 (2)	0.030	C(G2)	0.0960 (18)	0.4514 (17)	0.3307 (5)	0.056 (6)
P(2)	0.3344 (3)	−0.0142 (3)	0.3230 (2)	0.032	C(G3)	0.0311 (11)	0.4978 (13)	0.3803 (10)	0.081 (8)
P(3)	0.3838 (4)	0.2250 (4)	0.3367 (2)	0.034	C(G4)	0.0748 (20)	0.5450 (10)	0.4157 (10)	0.082 (8)
P(4)	0.2865 (4)	0.3841 (3)	0.2529 (2)	0.034	C(G5)	0.1834 (18)	0.5459 (17)	0.4014 (5)	0.076 (7)
P(5)	0.1227 (4)	0.3491 (3)	0.1429 (2)	0.034	C(G6)	0.2483 (11)	0.4995 (13)	0.3518 (10)	0.059 (6)
P(6)	0.0962 (3)	0.1568 (3)	0.1266 (2)	0.031	C(H1)	0.3374 (9)	0.4682 (11)	0.1926 (6)	0.036 (4)
F(11)	0.0280 (9)	0.2649 (8)	0.3852 (6)	0.070	C(H2)	0.4175 (17)	0.4391 (10)	0.1422 (12)	0.067 (7)
F(12)	−0.0556 (8)	0.2535 (9)	0.2793 (6)	0.069	C(H3)	0.4477 (18)	0.5003 (9)	0.0921 (10)	0.090 (8)
F(13)	0.0043 (10)	0.1009 (9)	0.3543 (6)	0.079	C(H4)	0.3978 (9)	0.5906 (11)	0.0923 (6)	0.063 (6)
F(21)	0.4995 (8)	0.0273 (7)	0.1625 (6)	0.058	C(H5)	0.3178 (17)	0.6197 (10)	0.1427 (12)	0.083 (8)
F(22)	0.5247 (10)	0.2068 (9)	0.1736 (6)	0.083	C(H6)	0.2876 (18)	0.5585 (9)	0.1929 (10)	0.060 (6)
F(23)	0.4354 (9)	0.1720 (10)	0.0794 (5)	0.079	C(I1)	0.0375 (19)	0.4566 (8)	0.1641 (11)	0.036 (5)
C(1)	0.3384 (13)	−0.0853 (12)	0.2588 (8)	0.035 (4)	C(I2)	−0.0595 (12)	0.4582 (8)	0.2058 (7)	0.064 (6)
C(2)	0.4059 (14)	0.3272 (14)	0.2837 (9)	0.044 (5)	C(I3)	−0.1195 (14)	0.5401 (8)	0.2260 (9)	0.077 (7)
C(3)	0.0319 (13)	0.2780 (12)	0.1331 (8)	0.033 (4)	C(I4)	−0.0824 (19)	0.6203 (8)	0.2045 (11)	0.085 (8)
C(4)	−0.278 (3)	0.300 (2)	0.109 (2)	0.129 (12)	C(I5)	0.0146 (12)	0.6187 (8)	0.1628 (7)	0.075 (7)
C(A1)	0.2722 (16)	−0.1001 (12)	0.1421 (6)	0.038 (5)	C(I6)	0.0746 (14)	0.5369 (8)	0.1426 (9)	0.063 (6)
C(A2)	0.3782 (12)	−0.1149 (15)	0.1113 (7)	0.047 (5)	C(J1)	0.1858 (14)	0.3771 (12)	0.0606 (5)	0.035 (4)
C(A3)	0.4062 (12)	−0.1462 (8)	0.0517 (9)	0.051 (5)	C(J2)	0.1228 (14)	0.4236 (11)	0.0193 (11)	0.054 (6)
C(A4)	0.3281 (16)	−0.1627 (12)	0.0229 (6)	0.061 (6)	C(J3)	0.1670 (10)	0.4365 (16)	−0.0442 (10)	0.063 (6)
C(A5)	0.2220 (12)	−0.1479 (15)	0.0537 (7)	0.052 (6)	C(J4)	0.2741 (14)	0.4030 (12)	−0.0664 (5)	0.070 (7)
C(A6)	0.1941 (12)	−0.1166 (8)	0.1133 (9)	0.044 (5)	C(J5)	0.3370 (14)	0.3565 (11)	−0.0251 (11)	0.068 (7)
C(B1)	0.1262 (7)	−0.1115 (8)	0.2578 (5)	0.029 (4)	C(J6)	0.2929 (10)	0.3435 (16)	0.0384 (10)	0.058 (6)
C(B2)	0.0275 (14)	−0.0677 (7)	0.2881 (9)	0.049 (5)	C(K1)	0.1686 (14)	0.1504 (10)	0.0439 (6)	0.031 (4)
C(B3)	−0.0484 (14)	−0.1178 (8)	0.3205 (10)	0.056 (6)	C(K2)	0.1273 (13)	0.2027 (10)	−0.0048 (10)	0.048 (5)
C(B4)	−0.0256 (7)	−0.2118 (8)	0.3226 (5)	0.060 (6)	C(K3)	0.1841 (9)	0.1974 (14)	−0.0663 (8)	0.063 (6)
C(B5)	0.0731 (14)	−0.2556 (7)	0.2923 (9)	0.058 (6)	C(K4)	0.2829 (14)	0.1398 (10)	−0.0790 (6)	0.050 (5)
C(B6)	0.1489 (14)	−0.2055 (8)	0.2599 (10)	0.043 (5)	C(K5)	0.3232 (13)	0.0874 (10)	−0.0303 (10)	0.048 (5)
C(C1)	0.2388 (11)	−0.0550 (9)	0.3898 (5)	0.033 (4)	C(K6)	0.2665 (9)	0.0927 (14)	0.0311 (8)	0.047 (5)
C(C2)	0.1988 (14)	−0.0002 (9)	0.4394 (7)	0.050 (5)	C(L1)	−0.0218 (9)	0.1047 (12)	0.1298 (6)	0.027 (4)
C(C3)	0.1338 (19)	−0.0312 (12)	0.4935 (8)	0.068 (7)	C(L2)	−0.1003 (17)	0.1123 (15)	0.1841 (5)	0.053 (6)
C(C4)	0.1088 (11)	−0.1170 (9)	0.4981 (5)	0.064 (6)	C(L3)	−0.1918 (14)	0.0766 (9)	0.1889 (8)	0.056 (6)
C(C5)	0.1488 (14)	−0.1718 (9)	0.4485 (7)	0.068 (7)	C(L4)	−0.2049 (9)	0.0334 (12)	0.1394 (6)	0.056 (6)
C(C6)	0.2138 (19)	−0.1409 (12)	0.3944 (8)	0.060 (6)	C(L5)	−0.1264 (17)	0.0258 (15)	0.0851 (5)	0.068 (7)
C(D1)	0.4653 (10)	−0.0648 (15)	0.3449 (11)	0.034 (4)	C(L6)	−0.0349 (14)	0.0615 (9)	0.0803 (8)	0.053 (6)
C(D2)	0.5572 (10)	−0.0559 (14)	0.3006 (7)	0.046 (5)	ClS(11)	0.6784 (18)	0.4129 (16)	0.3477 (11)	0.51 (2)[c]
C(D3)	0.6563 (11)	−0.0957 (6)	0.3136 (7)	0.055 (6)	ClS(12)	0.6588 (16)	0.3428 (15)	0.4798 (10)	0.54 (2)
C(D4)	0.6634 (10)	−0.1443 (15)	0.3710 (11)	0.068 (7)	ClS(13)	0.7599 (23)	0.4086 (23)	0.4473 (16)	0.38 (2)
C(D5)	0.5714 (10)	−0.1532 (14)	0.4154 (7)	0.062 (6)	ClS(14)	0.7555 (26)	0.4418 (24)	0.3763 (16)	0.35 (2)
C(D6)	0.4723 (11)	−0.1134 (6)	0.4023 (7)	0.044 (5)	ClS(15)	0.763 (3)	0.333 (3)	0.407 (2)	0.28 (2)
C(E1)	0.5193 (10)	0.1755 (16)	0.3521 (11)	0.035 (4)	ClS(21)	0.5474 (17)	0.3507 (15)	0.6601 (11)	0.51 (2)
C(E2)	0.5265 (9)	0.1133 (8)	0.4038 (7)	0.053 (6)	ClS(22)	0.4191 (18)	0.2917 (17)	0.7783 (11)	0.49 (2)
C(E3)	0.6249 (9)	0.0786 (14)	0.4195 (9)	0.068 (7)	ClS(23)	0.445 (4)	0.445 (4)	0.737 (2)	0.24 (2)
C(E4)	0.7161 (10)	0.1061 (16)	0.3834 (11)	0.064 (6)	ClS(24)	0.512 (3)	0.350 (3)	0.745 (2)	0.33 (2)
C(E5)	0.7089 (9)	0.1683 (8)	0.3317 (7)	0.062 (6)	ClS(25)	0.426 (3)	0.325 (3)	0.696 (2)	0.29 (2)
C(E6)	0.6105 (9)	0.2031 (14)	0.3161 (9)	0.059 (6)					

[a] Atoms C(4), Cl(1), and Cl(2) belong to the ordered solvent molecule, and ClS(11)–ClS(25) model the disorder of two solvent molecules. [b] For Pt, Sn, Cl, P, and F atoms U is the equivalent isotropic displacement parameter defines as $U = {}^1/_3\sum_{i=1,3}^{3}\sum_{j=1,3}^{3}U_{ij}b_ib_j(\mathbf{a}_i\cdot\mathbf{a}_j)$, where b_i is the ith reciprocal cell edge and $\mathbf{a}_i$ is the ith direct cell vector. [c] For ClS atoms U is the refined occupancy factor.

displacement parameters of their carbon atoms were allowed to vary. The refinement converged at $R = 0.051$ and $R_w = 0.059$.

The final atomic coordinates are listed in Table V. In the final difference electron density map the function values range from −2.6 to +3.2 e Å^{-3}, the extreme ones being associated with positions of the two partially revealed, disordered solvent molecules.

All calculations were performed by using the locally developed GX program package.[41] The neutral-atom scattering factors and anomalous dispersion corrections were taken from ref 42.

ESCA Analyses. The spectra were obtained on powdered samples pressed into copper foils by using a SSL SSX-100 instrument fitted with a Mg Kα X-ray source (1253.6 eV). Spectra were computer-fitted to 70% Gaussian line shapes, without using any constraints to the final fit, and binding energies were reproducible to within 0.1 eV. The carbon 1s binding energy at 285.0 eV was used to calibrate the spectra.

Acknowledgment. We thank the NSERC (Canada) for financial support (to R.J.P.), the SERC (U.K.) for a research studentship (G.D.), and NATO for a travel grant.

Supplementary Material Available: Listings of anisotropic displacement parameters, hydrogen atom coordinates, and bond lengths and angles (Tables VI–VIII) (6 pages); a listing of observed and calculated structure factor amplitudes (32 pages). Ordering information is given on any current masthead page.

(41) Mallinson, P. R.; Muir, K. W. *J. Appl. Crystallogr.* **1985**, *18*, 51.
(42) *International Tables for X-ray Crystallography*; Kynoch Press: Birmingham, England, 1974; Vol. IV.